

QCD corrections to Υ production via color-octet states at the Tevatron and LHC

Bin Gong^{1,2,3}, Jian-Xiong Wang^{1,3} and Hong-Fei Zhang^{1,3}

Institute of High Energy Physics, CAS, P.O. Box 918(4), Beijing, 100049, China.

Institute of Theoretical Physics, CAS, P.O. Box 2735, Beijing, 100190, China.

Theoretical Physics Center for Science Facilities, CAS, Beijing, 100049, China.

(Dated: September 21, 2010)

The NLO QCD corrections to Υ production via S-wave color-octet states $\Upsilon[S_0^{(8)}, S_1^{(8)}]$ at the Tevatron and LHC is calculated. The K factors of total cross section (ratio of NLO to LO) are 1.313 and 1.379 for $\Upsilon[S_0^{(8)}]$ and $\Upsilon[S_1^{(8)}]$ at the Tevatron, while at the LHC they are 1.044 and 1.182, respectively. By fitting the experimental data from the D0, the matrix elements for S-wave color-octet states are obtained. And new predictions for Υ production are presented. The prediction for the polarization of inclusive Υ contains large uncertainty rising from the polarization of Υ from feed-down of χ_b . To further clarify the situation, new measurements on the production and polarization for direct Υ are expected.

PACS numbers: 12.38.Bx, 13.25.Gv, 13.60.Le

I. INTRODUCTION

For heavy quarkonium production and decay, a naive perturbative QCD and nonrelativistic factorization treatment is applied straightforwardly. It is called color-singlet mechanism (CSM). To describe the huge discrepancy of the high- p_t J/ψ production between the theoretical prediction based on CSM and the experimental measurement at Tevatron, a color-octet mechanism [1] was proposed based on the non-relativistic QCD (NRQCD) [2]. In the application, J/ψ or Υ related productions or decays are very good places for two reasons, theoretically charm and bottom quarks are thought to be heavy enough, so that charmonium and bottomonium can be treated within the NRQCD framework, experimentally there is a very clear signal to detect J/ψ and Υ . The key point is that the color-octet mechanism depends on nonperturbative universal NRQCD matrix elements, which is obtained by fitting the data. Therefore various efforts have been made to confirm this mechanism, or to fix the magnitudes of the universal NRQCD matrix elements. Although it seems to show qualitative agreements with experimental data, there are certain difficulties. A review of the situation could be found in Refs. [3, 4].

To explain the experimental measurements [5, 6] of J/ψ production at the B factories, a series of calculations [7, 8] in the CSM reveal that the next-to-leading order (NLO) QCD corrections give the main contribution to the related processes. Together with the relativistic correction [9], it seems that most experimental data for J/ψ production at the B factories could be understood. Recent studies show that the NLO QCD correction also plays an important role in J/ψ production at RHIC [10] and the hadroproduction of χ_c [11]. For the J/ψ photoproduction, the p_t and z distributions can be described by the NLO calculations in CSM [12] by choosing a small renormalization scale, but recent NLO calculations in CSM [13] show that the p_t distributions of the production and polarization for J/ψ can not be well described when choosing a proper renormalization scale. Although the

complete calculation at NLO in COM [14] can account for the experimental measurements on the p_t distribution, it cannot extend to J/ψ polarization case. To further study the heavy quarkonium production mechanism, there are many other efforts performed, such as NLO QCD correction to J/ψ production associated with photon [15], QED contributions in J/ψ hadroproduction [16], inclusive J/ψ production from Υ decay [17], double heavy quarkonium hadronproduction [18], and NLO QCD correction to J/ψ production from Z decay [19].

For the polarized heavy quarkonium hadroproduction, the leading order (LO) NRQCD prediction gives a sizable transverse polarization for J/ψ production at high p_t at Tevatron while the experimental measurement [20] gives slight longitudinal polarized result. The discrepancy was also found in Υ production. In a recent paper [21], the measurement on polarization of Υ production at Tevatron is presented and the NRQCD prediction [22] is not coincide with it. Within the NRQCD framework, higher order correction is thought to be an important way towards the solution of such puzzles. Recently, NLO QCD corrections to J/ψ and Υ hadroproduction have been calculated [23–27], and the results show that the NLO QCD corrections give significant enhancement to both total cross section and momentum distribution for the color-singlet channel. This would reduce the contribution of color-octet channel in the production. Also, it is found in Ref. [24] that the polarizations for J/ψ and Υ hadroproduction via color-singlet channel would change drastically from transverse polarization dominant at LO into longitudinal polarization dominant in the whole range of the transverse momentum p_t at NLO. It seems that these results open a door to the solution of the problem. But things are not always going as expected. The NLO QCD corrections to the J/ψ production via S-wave color-octet states were studied in our previous work [28]. It was found that the effect of NLO QCD correction is small and the discrepancy holds on. For the color-singlet part, the partial next-to-next-to-leading order (NNLO) calculations for Υ and J/ψ hadroproduction show that the un-

certainty from higher order QCD correction [38] is quite large, therefore no definite conclusion can be made. As we know, the contribution from the color-octet states is smaller in the Υ production than that in J/ψ production, thus things may be different. In this paper, we present our calculation on NLO QCD corrections to Υ hadroproduction via S-wave color-octet states. New matrix elements are fitted and new prediction for the polarization status is presented.

This paper is organized as follows. In Sec. II, we give the LO cross section for the process. The calculation of NLO QCD corrections are described in Sec. III. In Sec. IV, we present the formula in final integration to obtain the transverse momentum distribution of Υ production. Sec. V. is devoted to the description about the calculation of Υ polarization. The treatment of J/ψ is discussed in Sec. VI. The numerical results are presented in Sec. VII, while the summary and discussion are given in Sec. VIII. In the Appendix, several details of the calculation are presented.

II. THE LO CROSS SECTION

According to the NRQCD factorization formalism, the inclusive cross section for direct Υ production in hadron-hadron collision is expressed as

$$\sigma[pp \rightarrow \Upsilon + X] = \sum_{i,j,k,n} \int dx_1 dx_2 G_{i/p} G_{j/p} \times \hat{\sigma}[i + j \rightarrow (b\bar{b})_n + k] \langle \mathcal{O}_n^H \rangle, \quad (1)$$

where p is either a proton or an anti-proton, the indices i, j, k run over all the partonic species and n denotes the color, spin and angular momentum states of the intermediate $b\bar{b}$ pair. The short-distance contribution $\hat{\sigma}$ can be perturbatively calculated order by order in α_s . The hadronic matrix elements $\langle \mathcal{O}_n^H \rangle$ are related to the hadronization from the state $(b\bar{b})_n$ into Υ which are fully governed by the non-perturbative QCD effects. In the following, $\hat{\sigma}$ represents the corresponding partonic cross section.

At LO, there are three partonic processes:

$$g(p_1) + g(p_2) \rightarrow \Upsilon[{}^1S_0^{(8)}, {}^3S_1^{(8)}](p_3) + g(p_4), \quad (L1)$$

$$g(p_1) + q(p_2) \rightarrow \Upsilon[{}^1S_0^{(8)}, {}^3S_1^{(8)}](p_3) + q(p_4), \quad (L2)$$

$$q(p_1) + \bar{q}(p_2) \rightarrow \Upsilon[{}^1S_0^{(8)}, {}^3S_1^{(8)}](p_3) + g(p_4). \quad (L3)$$

where q represents a sum over all possible light quarks or anti-quarks: $u, d, s, c, \bar{u}, \bar{d}, \bar{s}$ and \bar{c} . In our calculation of Υ production, we take charm quark as light quark as an approximation. Typical Feynman diagrams for these three processes are shown in Fig. 1. And the partonic differential cross sections in $n = 4 - 2\epsilon$ dimension for LO processes can be obtained as

$$\begin{aligned} \frac{d\hat{\sigma}^B(q\bar{q} \rightarrow \Upsilon[{}^3S_1^{(8)}]g)}{d\hat{t}} &= \frac{\pi^2 \alpha_s^3 \langle \mathcal{O}_8^\Upsilon({}^3S_1) \rangle [(\hat{t}-1)^2 + (\hat{u}-1)^2] [4\hat{t}^2 - \hat{t}\hat{u} + 4\hat{u}^2]}{324m_b^5 \hat{s}^2 (\hat{s}-1)^2 \hat{t}\hat{u}} + \mathcal{O}(\epsilon), \\ \frac{d\hat{\sigma}^B(gq \rightarrow \Upsilon[{}^3S_1^{(8)}]q)}{d\hat{t}} &= \frac{-\pi^2 \alpha_s^3 \langle \mathcal{O}_8^\Upsilon({}^3S_1) \rangle [(\hat{s}-1)^2 + (\hat{u}-1)^2] [4\hat{s}^2 - \hat{s}\hat{u} + 4\hat{u}^2]}{864m_b^5 \hat{s}^3 (\hat{t}-1)^2 \hat{u}} + \mathcal{O}(\epsilon), \\ \frac{d\hat{\sigma}^B(gg \rightarrow \Upsilon[{}^3S_1^{(8)}]g)}{d\hat{t}} &= \frac{\pi^2 \alpha_s^3 \langle \mathcal{O}_8^\Upsilon({}^3S_1) \rangle [(\hat{s}^2-1)^2 + (\hat{t}^2-1)^2 + (\hat{u}^2-1)^2 - 6\hat{s}\hat{t}\hat{u} - 2][19 - 27(\hat{s}\hat{t} + \hat{t}\hat{u} + \hat{u}\hat{s})]}{1152m_b^5 \hat{s}^2 (\hat{t}-1)^2 (\hat{u}-1)^2 (\hat{s}-1)^2} + \mathcal{O}(\epsilon), \\ \frac{d\hat{\sigma}^B(q\bar{q} \rightarrow \Upsilon[{}^1S_0^{(8)}]g)}{d\hat{t}} &= \frac{5\pi^2 \alpha_s^3 \langle \mathcal{O}_8^\Upsilon({}^1S_0) \rangle [\hat{t}^2 + \hat{u}^2]}{216m_b^5 \hat{s}^3 (\hat{s}-1)^2} + \mathcal{O}(\epsilon), \\ \frac{d\hat{\sigma}^B(gq \rightarrow \Upsilon[{}^1S_0^{(8)}]q)}{d\hat{t}} &= \frac{-5\pi^2 \alpha_s^3 \langle \mathcal{O}_8^\Upsilon({}^1S_0) \rangle [\hat{s}^2 + \hat{u}^2]}{576m_b^5 \hat{s}^2 \hat{t} (\hat{t}-1)^2} + \mathcal{O}(\epsilon), \\ \frac{d\hat{\sigma}^B(gg \rightarrow \Upsilon[{}^1S_0^{(8)}]g)}{d\hat{t}} &= \frac{5\pi^2 \alpha_s^3 \langle \mathcal{O}_8^\Upsilon({}^1S_0) \rangle [\hat{s}^2 \hat{t}^2 + \hat{s}^2 \hat{u}^2 + \hat{t}^2 \hat{u}^2 + \hat{s}\hat{t}\hat{u}][\hat{s}^4 + \hat{t}^4 + \hat{u}^4 + 1]}{256m_b^5 \hat{s}^3 \hat{t}\hat{u} (\hat{t}-1)^2 (\hat{u}-1)^2 (\hat{s}-1)^2} + \mathcal{O}(\epsilon), \end{aligned} \quad (2)$$

by introducing three dimensionless kinematic variables:

$$\hat{s} = \frac{(p_1 + p_2)^2}{4m_b^2}, \quad \hat{t} = \frac{(p_1 - p_3)^2}{4m_b^2}, \quad \hat{u} = \frac{(p_1 - p_4)^2}{4m_b^2}, \quad (3)$$

and the reasonable approximation $M_\Upsilon = 2m_b$ is taken. Our LO results are consistent with those in Ref. [29]. The LO total cross section is obtained by convoluting

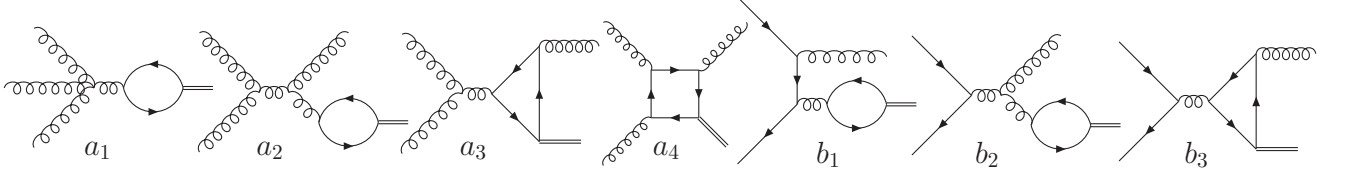


FIG. 1: Typical Feynman diagrams for LO processes. *a*) Feynman diagrams for process (L1); *b*) Feynman diagrams for processes (L2) and (L3). Diagrams in groups (*a*₁), (*a*₂), (*b*₁) and (*b*₂) are absent for the $^1S_0^{(8)}$ state.

the partonic cross section with the parton distribution function (PDF) in the proton:

$$\sigma^B[pp \rightarrow \Upsilon^{(8)} + X] = \sum_{i,j,k} \int \hat{\sigma}^B[i + j \rightarrow \Upsilon^{(8)} + k] \quad (4)$$

$$\times G_{i/p}(x_1, \mu_f) G_{j/p}(x_2, \mu_f) dx_1 dx_2,$$

where $\Upsilon^{(8)}$ denotes certain color-octet $\Upsilon[^1S_0^{(8)}]$ or $\Upsilon[^3S_1^{(8)}]$, μ_f is the factorization scale.

III. THE NLO CROSS SECTION

The NLO contributions can be written as a sum of two parts: first is the virtual corrections which arise from loop diagrams, the other is the real corrections caused by radiation of a real gluon, or a gluon splitting into a light quark-antiquark pair, or a light (anti)quark splitting into a light (anti) quark and a gluon.

A. Virtual corrections

There exist ultraviolet (UV), infrared (IR) and Coulomb singularities in the calculation of the virtual corrections. UV divergences from self-energy and triangle diagrams are canceled by introducing renormalization. Here we adopt the renormalization scheme used in Ref. [30]. The renormalization constants Z_m , Z_2 , Z_{2l} and Z_3 which correspond to bottom quark mass m_b , bottom-field ψ_b , light quark field ψ_q and gluon field A_μ^a are defined in the on-mass-shell (OS) scheme while Z_g for the QCD gauge coupling constant α_s is defined in the modified-minimal-subtraction ($\overline{\text{MS}}$) scheme:

$$\begin{aligned} \delta Z_m^{OS} &= -3C_F \frac{\alpha_s}{4\pi} \left[\frac{1}{\epsilon_{UV}} - \gamma_E + \ln \frac{4\pi\mu_r^2}{m_b^2} + \frac{4}{3} \right], \\ \delta Z_2^{OS} &= -C_F \frac{\alpha_s}{4\pi} \left[\frac{1}{\epsilon_{UV}} + \frac{2}{\epsilon_{IR}} - 3\gamma_E + 3 \ln \frac{4\pi\mu_r^2}{m_b^2} + 4 \right], \\ \delta Z_{2l}^{OS} &= -C_F \frac{\alpha_s}{4\pi} \left[\frac{1}{\epsilon_{UV}} - \frac{1}{\epsilon_{IR}} \right], \\ \delta Z_3^{OS} &= \frac{\alpha_s}{4\pi} \left[(\beta_0 - 2C_A) \left(\frac{1}{\epsilon_{UV}} - \frac{1}{\epsilon_{IR}} \right) \right], \\ \delta Z_g^{\overline{\text{MS}}} &= -\frac{\beta_0}{2} \frac{\alpha_s}{4\pi} \left[\frac{1}{\epsilon_{UV}} - \gamma_E + \ln(4\pi) \right], \end{aligned} \quad (5)$$

where γ_E is the Euler's constant, $\beta_0 = \frac{11}{3}C_A - \frac{4}{3}T_F n_f$ is the one-loop coefficient of the QCD beta function and n_f is the number of active quark flavors. We have four light quarks u , d , s and c in our calculation, so $n_f=4$. The color factors are given by $T_F = 1/2$, $C_F = 4/3$, $C_A = 3$ and μ_r is the renormalization scale.

There are 267 (for the $^1S_0^{(8)}$ state) and 413 (for the $^3S_1^{(8)}$ state) NLO diagrams for process (L1), including counter-term diagrams, while for both processes (L2) and (L3), there are 49 (for the $^1S_0^{(8)}$ state) and 111 (for the $^3S_1^{(8)}$ state) NLO diagrams. Part of the Feynman diagrams for these processes are shown in Fig. 2. The diagrams in which a virtual gluon line connects the quark pair possess Coulomb singularities, which can be isolated and attributed into renormalization of the $b\bar{b}$ wave function.

For each process, by summing over contributions from all diagrams, the virtual correction to the differential cross section can be expressed as

$$\frac{d\hat{\sigma}_{[L_i]}^V}{dt} \propto 2\text{Re} \left(M_{[L_i]}^B M_{[L_i]}^{V*} \right), \quad (6)$$

where $M_{[L_i]}^B$ is the amplitude of process (L_i) at LO, and $M_{[L_i]}^V$ is the renormalized amplitude of corresponding process at NLO. $M_{[L_i]}^V$ is UV and Coulomb finite, but it still contains IR divergences. And the total cross section of virtual contribution could be written as

$$\sigma^V[pp \rightarrow \Upsilon^{(8)} + X] = \sum_{i,j,k} \int \hat{\sigma}^V[i + j \rightarrow \Upsilon^{(8)} + k] \quad (7)$$

$$\times G_{i/p}(x_1, \mu_f) G_{j/p}(x_2, \mu_f) dx_1 dx_2,$$

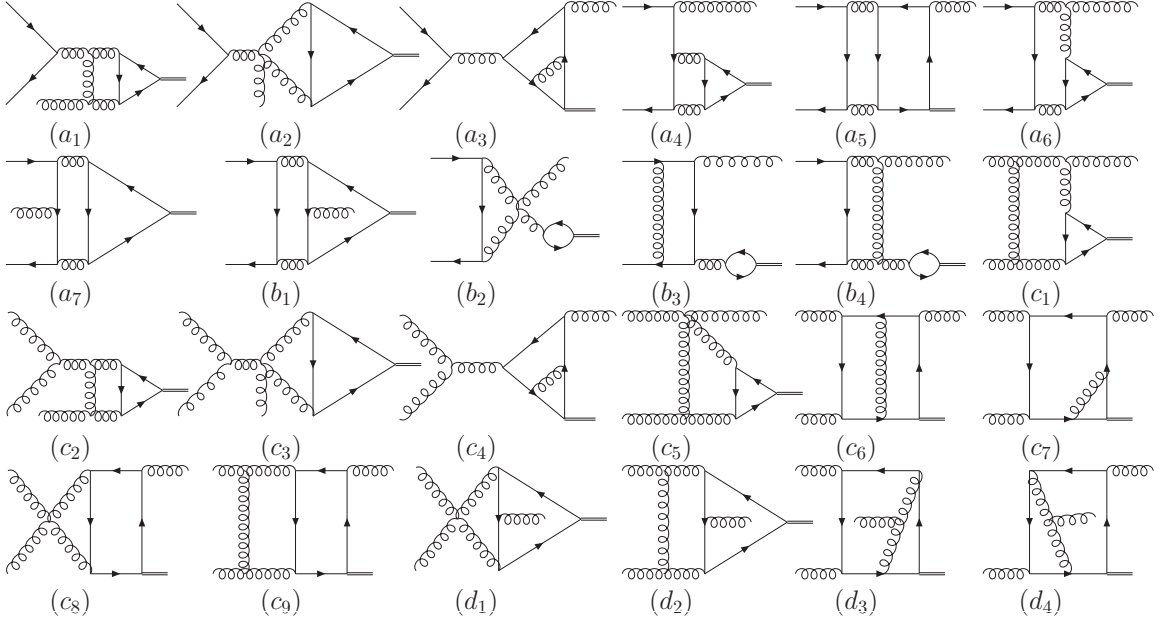


FIG. 2: Typical one-loop diagrams. *a*) Feynman diagrams for $gq \rightarrow \Upsilon[S_0^{(8)}]q$ and $q\bar{q} \rightarrow \Upsilon[S_0^{(8)}]g$; *a* + *b*) Feynman diagrams for $gq \rightarrow \Upsilon[S_1^{(8)}]q$ and $q\bar{q} \rightarrow \Upsilon[S_1^{(8)}]g$; *c*) Feynman diagrams for $gg \rightarrow \Upsilon[S_0^{(8)}]g$; *c* + *d*) Feynman diagrams for $gg \rightarrow \Upsilon[S_1^{(8)}]g$. Counter-term diagrams, together with corresponding loop diagrams, are not shown here.

B. Real corrections

There are eight processes involved in the real corrections:

$$gg \rightarrow \Upsilon[S_0^{(8)}, S_1^{(8)}]gg, \quad (R1)$$

$$gq \rightarrow \Upsilon[S_0^{(8)}, S_1^{(8)}]gq, \quad (R2)$$

$$q\bar{q} \rightarrow \Upsilon[S_0^{(8)}, S_1^{(8)}]gg, \quad (R3)$$

$$gg \rightarrow \Upsilon[S_0^{(8)}, S_1^{(8)}]q\bar{q}, \quad (R4)$$

$$q\bar{q} \rightarrow \Upsilon[S_0^{(8)}, S_1^{(8)}]q\bar{q}, \quad (R5)$$

$$q\bar{q} \rightarrow \Upsilon[S_0^{(8)}, S_1^{(8)}]q'\bar{q}', \quad (R6)$$

$$qq \rightarrow \Upsilon[S_0^{(8)}, S_1^{(8)}]qq, \quad (R7)$$

$$qq' \rightarrow \Upsilon[S_0^{(8)}, S_1^{(8)}]qq', \quad (R8)$$

where q, q' denote light quarks (anti-quarks) with different flavors. Feynman diagrams for these processes are shown in Fig. 3. We have neglected the contributions from the another two processes, $gg \rightarrow \Upsilon^{(8)}b\bar{b}$ and $q\bar{q} \rightarrow \Upsilon^{(8)}b\bar{b}$, which are IR finite and small. Phase space integrations of above eight processes generate IR singularities, which are either soft or collinear and can be conveniently isolated by slicing the phase space into different regions. We use the two-cut-off phase space slicing method [31], which introduces two small cutoffs to decompose the phase space into three parts. Then the real cross section can be written as

$$\sigma^R = \sigma^S + \sigma^{HC} + \sigma^{H\bar{C}}. \quad (8)$$

It is easy to observe that different parts of IR singularities from one real process may be factorized and each part should be added into the cross sections of different LO processes. This is the reason why we have to calculate the NLO corrections to the three LO processes together.

1. soft

Soft singularities arise from real gluon emission. Thus only real processes (R1), (R2) and (R3) contain soft singularities, corresponding to the three LO processes. One should notice that, unlike color-singlet case, the soft singularities caused by emitting a soft gluon from the quark pair in the S-wave color octet exists and we find that the factorized matrix element is the same as the case of emitting a soft gluon from a gluon.

Suppose p_5 is the momentum of the emitted gluon. If we define the Mandelstam invariants as $s_{ij} = (p_i + p_j)^2$ and $t_{ij} = (p_i - p_j)^2$, the soft region is defined in term of the energy of p_5 in the $p_1 + p_2$ rest frame by $0 \leq E_5 \leq \delta_s \sqrt{s_{12}}/2$. For each of the three real processes, $\hat{\sigma}^S$ from the soft regions is calculated analytically under the soft approximation.

Following the similar factorization procedure as applied in the calculation of color-singlet case [25], the matrix elements for a certain real process (R_i) in the soft region can be written as

$$|M_{[R_i]}|^2|_{\text{soft}} \simeq -4\pi\alpha_s\mu_r^{2\epsilon} \sum_{j,k=1}^4 \frac{-p_j \cdot p_k}{(p_j \cdot p_5)(p_k \cdot p_5)} M_{[L_i]}^{jk}, \quad (9)$$

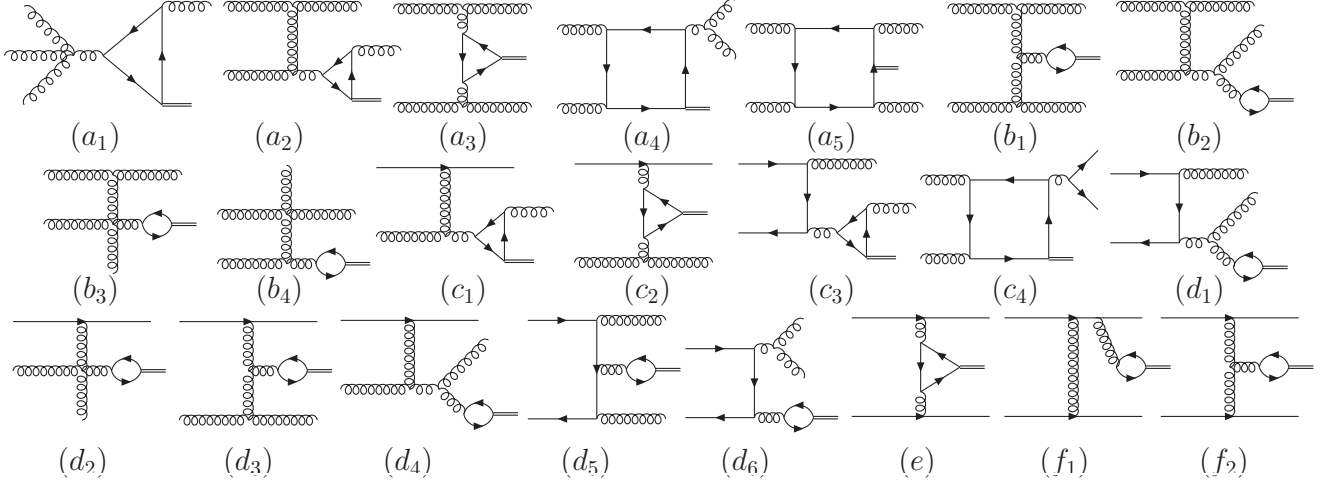


FIG. 3: Feynman diagrams for real correction processes. *a*) R1 ($\Upsilon[S_0^{(8)}]$); *a* + *b*) R1 ($\Upsilon[S_1^{(8)}]$); *c*) R2~R4 ($\Upsilon[S_0^{(8)}]$); *c* + *d*) R2~R4 ($\Upsilon[S_1^{(8)}]$); *e*) R5~R8 ($\Upsilon[S_0^{(8)}]$); *e* + *f*) R5~R8 ($\Upsilon[S_1^{(8)}]$). R1 ($\Upsilon[S_0^{(8)}]$) denotes process $gg \rightarrow \Upsilon[S_0^{(8)}]gg$, R1 ($\Upsilon[S_1^{(8)}]$) denotes process $gg \rightarrow \Upsilon[S_1^{(8)}]gg$, and so on.

with

$$M_{[L_i]}^{jk} = [\mathbf{T}^a(j) \mathbf{M}_{[L_i]}^{b_1 \dots b_{j'} \dots b_4}]^\dagger [\mathbf{T}^a(k) \mathbf{M}_{[L_i]}^{b_1 \dots b_{k'} \dots b_4}] \quad (10)$$

where $\mathbf{M}_{[L_i]}^{b_1 \dots b_4}$ is the color connected Born matrix element for LO processes (L_i). If the emitting parton j is an initial state quark or a final state antiquark, $\mathbf{T}^a(j) = T_{b_{j'} b_j}^a$. For an initial state antiquark or a final state quark $\mathbf{T}^a(j) = -T_{b_j b_{j'}}^a$. If the emitting parton j is a gluon or the color-octet state, $\mathbf{T}^a(j) = i f_{ab_j b_{j'}}$. And the corresponding parton level differential cross section can be expressed as

$$d\hat{\sigma}_{[L_i]}^S = \left[\frac{\alpha_s}{2\pi} \frac{\Gamma(1-\epsilon)}{\Gamma(1-2\epsilon)} \left(\frac{4\pi\mu_r^2}{s_{12}} \right)^\epsilon \right] \sum_{j,k=1}^4 d\hat{\sigma}_{[L_i]}^{jk} I^{jk}, \quad (11)$$

with

$$d\hat{\sigma}_{[L_i]}^{jk} = \frac{1}{2\Phi} \overline{\sum} M_{[L_i]}^{jk} d\Gamma_2. \quad (12)$$

The factor I^{jk} is universal for all three real processes, and is given in Appendix. (A). Sometimes $d\hat{\sigma}_{[L_i]}^{jk}$ may be written in a more compact form as

$$d\hat{\sigma}_{[L_i]}^{jk} = C_{[L_i]}^{jk} d\hat{\sigma}_{[L_i]}^B, \quad (13)$$

where $C_{[L_i]}^{jk}$ is a constant. This is always true if the LO process (L_i) contain only one independent color factor in the matrix element. But for processes with two or more than two independent color factors, there seems no sure reason for it to be or not to be true. Of course, no matter Eq. (13) is true or not, we can always obtain $d\hat{\sigma}_{[L_i]}^{jk}$ through Eq. (12). Most processes involved in this calculation have more than one independent color factors, and they are listed in Appendix. (B1).

2. hard collinear

The hard collinear regions of the phase space are those where any invariant (s_{ij} or t_{ij}) becomes smaller in magnitude than $\delta_c s_{12}$. It is treated according to whether the singularities are from initial or final state emitting or splitting in the origin.

a. final state collinear For real processes (R1) ~ (R6), which contain final state collinear singularities, the final state collinear region is defined by $0 \leq s_{45} \leq \delta_c s_{12}$. Again following the similar factorization procedure described in Ref [31], the parton level cross section in the hard final state collinear region can be expressed as

$$\hat{\sigma}_f^{HC}[R_i] = \hat{\sigma}^B[L'_i] \left[\frac{\alpha_s}{2\pi} \frac{\Gamma(1-\epsilon)}{\Gamma(1-2\epsilon)} \left(\frac{4\pi\mu_r^2}{s_{12}} \right)^\epsilon \right] A_i^{HC}. \quad (14)$$

For a certain real process (R_i), (L'_i) is the corresponding LO process it factorizes into. And the coefficient A_i^{HC} are listed in Table. I, with

$$\begin{aligned} A_1^{g \rightarrow gg} &= N(11/6 + 2 \ln \delta'_s) \\ A_0^{g \rightarrow gg} &= N[67/18 - \pi^2/3 - \ln^2 \delta'_s - \ln \delta_c(11/6 + 2 \ln \delta'_s)] \\ A_1^{q \rightarrow qg} &= C_F(3/2 + 2 \ln \delta'_s) \\ A_0^{q \rightarrow qg} &= C_F[7/2 - \pi^2/3 - \ln^2 \delta'_s - \ln \delta_c(3/2 + 2 \ln \delta'_s)] \\ A_1^{g \rightarrow q\bar{q}} &= -n_f/3 \\ A_0^{g \rightarrow q\bar{q}} &= n_f/3(\ln \delta_c - 5/3), \end{aligned} \quad (15)$$

and

$$\delta'_s = \frac{s_{12}}{s_{12} + s_{45} - M_\Upsilon^2} \simeq \frac{\hat{s}}{\hat{s} - 1} \delta_s. \quad (16)$$

Thus the total cross section for real correction processes in hard final state collinear region can be written as:

$$\begin{aligned}\sigma_f^{HC} &= \sum_{i,j,k_1,k_2} \int \hat{\sigma}_f^{HC}[i+j \rightarrow \Upsilon^{(8)} + k_1 + k_2] \\ &\quad \times G_{i/p}(x_1, \mu_f) G_{j/p}(x_2, \mu_f) dx_1 dx_2 \\ &= \sum_{i,j,k} \int \hat{\sigma}^B[i+j \rightarrow \Upsilon^{(8)} + k] B^{HC}(k) \\ &\quad \times G_{i/p}(x_1, \mu_f) G_{j/p}(x_2, \mu_f) dx_1 dx_2, \quad (17)\end{aligned}$$

where

$$\begin{aligned}B^{HC}(g) &= \left[\frac{\alpha_s}{2\pi} \frac{\Gamma(1-\epsilon)}{\Gamma(1-2\epsilon)} \left(\frac{4\pi\mu_r^2}{s_{12}} \right)^\epsilon \right] \\ &\quad \times \left(\frac{A_1^{g \rightarrow gg} + A_1^{g \rightarrow q\bar{q}}}{\epsilon} + A_0^{g \rightarrow gg} + A_0^{g \rightarrow q\bar{q}} \right), \\ B^{HC}(q) &= \left[\frac{\alpha_s}{2\pi} \frac{\Gamma(1-\epsilon)}{\Gamma(1-2\epsilon)} \left(\frac{4\pi\mu_r^2}{s_{12}} \right)^\epsilon \right] \left(\frac{A_1^{q \rightarrow qq}}{\epsilon} + A_0^{q \rightarrow qq} \right).\end{aligned} \quad (18)$$

R_i	L'_i	A_i^{HC}
$gg \rightarrow \Upsilon^{(8)} gg$	$gg \rightarrow \Upsilon^{(8)} g$	$\frac{1}{\epsilon} A_1^{g \rightarrow gg} + A_0^{g \rightarrow gg}$
$gq \rightarrow \Upsilon^{(8)} gq$	$gq \rightarrow \Upsilon^{(8)} q$	$\frac{1}{\epsilon} A_1^{q \rightarrow qq} + A_0^{q \rightarrow qq}$
$gg \rightarrow \Upsilon^{(8)} q\bar{q}$	$gg \rightarrow \Upsilon^{(8)} g$	$\frac{1}{\epsilon} A_1^{g \rightarrow q\bar{q}} + A_0^{g \rightarrow q\bar{q}}$
$q\bar{q} \rightarrow \Upsilon^{(8)} gg$	$q\bar{q} \rightarrow \Upsilon^{(8)} g$	$\frac{1}{\epsilon} A_1^{g \rightarrow gg} + A_0^{g \rightarrow gg}$
$q\bar{q} \rightarrow \Upsilon^{(8)} q\bar{q}$	$q\bar{q} \rightarrow \Upsilon^{(8)} g$	$\frac{1}{n_f} \left(\frac{1}{\epsilon} A_1^{g \rightarrow q\bar{q}} + A_0^{g \rightarrow q\bar{q}} \right)$
$q\bar{q} \rightarrow \Upsilon^{(8)} q' \bar{q}'$	$q\bar{q} \rightarrow \Upsilon^{(8)} g$	$\left(1 - \frac{1}{n_f} \right) \left(\frac{1}{\epsilon} A_1^{g \rightarrow q\bar{q}} + A_0^{g \rightarrow q\bar{q}} \right)$

TABLE I: The hard final state collinear factors for real correction processes and the corresponding LO processes.

b. initial state collinear Almost all real processes, except process (R6), contain hard initial state collinear singularities. These singularities are partly absorbed into the redefinition of the parton distribution function (PDF) of the concerned hadrons (usually it is called as the mass factorization [32]). Here we adopt the scale dependent PDF using the $\overline{\text{MS}}$ convention given in Ref [31].

$$\begin{aligned}G_{b/p}(x, \mu_f) &= G_{b/p}(x) - \frac{1}{\epsilon} \left[\frac{\alpha_s}{2\pi} \frac{\Gamma(1-\epsilon)}{\Gamma(1-2\epsilon)} \left(\frac{4\pi\mu_r^2}{\mu_f^2} \right)^\epsilon \right] \\ &\quad \times \int_x^1 \frac{dz}{z} P_{bb'}(z) G_{b'/p}(x/z). \quad (19)\end{aligned}$$

The second term is sometimes referred as the mass factorization counter-term. There is still something remaining after the cancellation, which can be expressed in two terms. The first one, which only exists in the real processes with final state gluon, can be expressed as

$$\hat{\sigma}_i^{HC}[R_i] = \hat{\sigma}^B[L_i] \left[\frac{\alpha_s}{2\pi} \frac{\Gamma(1-\epsilon)}{\Gamma(1-2\epsilon)} \left(\frac{4\pi\mu_r^2}{\mu_f^2} \right)^\epsilon \right] A_i^{SC},$$

with

$$\begin{aligned}A_1^{SC} &= 2A^{SC}(g \rightarrow gg) \\ A_2^{SC} &= A^{SC}(q \rightarrow qq) + A^{SC}(g \rightarrow gg) \\ A_3^{SC} &= 2A^{SC}(q \rightarrow qq),\end{aligned} \quad (20)$$

and

$$\begin{aligned}A^{SC}(q \rightarrow qq) &= \frac{1}{\epsilon} C_F [3/2 + 2 \ln(\delta_s)] \\ A^{SC}(g \rightarrow gg) &= \frac{1}{\epsilon} [2N \ln \delta_s + (11N - 2n_f)/6].\end{aligned} \quad (21)$$

The corresponding hadronic total cross section is

$$\begin{aligned}\sigma_i^{HC} &= \sum_{i,j,k} \int \hat{\sigma}_i^{HC}[i+j \rightarrow \Upsilon^{(8)} + k + g] \\ &\quad \times G_{i/p}(x_1, \mu_f) G_{j/p}(x_2, \mu_f) dx_1 dx_2 \\ &= \sum_{i,j,k} \int \hat{\sigma}^B[i+j \rightarrow \Upsilon^{(8)} + k] [B^{SC}(i) + B^{SC}(j)] \\ &\quad \times G_{i/p}(x_1, \mu_f) G_{j/p}(x_2, \mu_f) dx_1 dx_2, \quad (22)\end{aligned}$$

with

$$\begin{aligned}B^{SC}(g) &= \left[\frac{\alpha_s}{2\pi} \frac{\Gamma(1-\epsilon)}{\Gamma(1-2\epsilon)} \left(\frac{4\pi\mu_r^2}{\mu_f^2} \right)^\epsilon \right] A^{SC}(g \rightarrow gg) \\ B^{SC}(q) &= \left[\frac{\alpha_s}{2\pi} \frac{\Gamma(1-\epsilon)}{\Gamma(1-2\epsilon)} \left(\frac{4\pi\mu_r^2}{\mu_f^2} \right)^\epsilon \right] A^{SC}(q \rightarrow qq).\end{aligned}$$

The other term is obtained by summing up the remaining contributions from all the real correction processes. It can be written as

$$\begin{aligned}\sigma_{add}^{HC}[pp \rightarrow \Upsilon^{(8)} + X] &\quad (23) \\ &\equiv \sum_{i,j,k} \int \hat{\sigma}^B[ij \rightarrow \Upsilon^{(8)} + k] \left[\frac{\alpha_s}{2\pi} \frac{\Gamma(1-\epsilon)}{\Gamma(1-2\epsilon)} \left(\frac{4\pi\mu_r^2}{s_{12}} \right)^\epsilon \right] \\ &\quad \times \left[G_{i/p}(x_1, \mu_f) \tilde{G}_{j/p}(x_2, \mu_f) + (x_1 \leftrightarrow x_2) \right] dx_1 dx_2,\end{aligned}$$

with

$$\tilde{G}_{c/p}(x, \mu_f) = \sum_{c'} \int_x^{1-\delta_s \delta_{cc'}} \frac{dy}{y} G_{c'/p}(x/y, \mu_f) \tilde{P}_{cc'}(y), \quad (24)$$

and

$$\tilde{P}_{ij}(y) = P_{ij}(y) \ln \left(\delta_c \frac{1-y}{y} \frac{s_{12}}{\mu_f^2} \right) - P'_{ij}(y). \quad (25)$$

The n -dimensional unregulated ($y < 1$) splitting functions $P_{ij}(y, \epsilon)$ has been written as $P_{ij}(y, \epsilon) = P_{ij}(y) +$

$\epsilon P'_{ij}(y)$ with

$$\begin{aligned}
P_{qq}(y) &= C_F \frac{1+y^2}{1-y}, \\
P'_{qq}(y) &= -C_F(1-y), \\
P_{gq}(y) &= C_F \frac{1+(1-y)^2}{y}, \\
P'_{gq}(y) &= -C_F y, \\
P_{gg}(y) &= 2N \left[\frac{y}{1-y} + \frac{1-y}{y} + y(1-y) \right], \\
P'_{gg}(y) &= 0, \\
P_{qg}(y) &= \frac{1}{2} [y^2 + (1-y)^2], \\
P'_{qg}(y) &= -y(1-y).
\end{aligned} \tag{26}$$

C. Cross section of all NLO contributions

The hard noncollinear part $\sigma^{H\bar{C}}$ is IR finite and can be numerically computed using the standard Monte-Carlo integration techniques. Now the real cross section can be expressed as

$$\sigma^R = \sigma^S + \sigma_f^{HC} + \sigma_i^{HC} + \sigma_{add}^{HC} + \sigma^{H\bar{C}}. \tag{27}$$

And we have

$$\sigma^{NLO} = \sigma^B + \sigma^V + \sigma^R. \tag{28}$$

IV. TRANSVERSE MOMENTUM DISTRIBUTION

To obtain the transverse momentum p_t distribution of Υ , a similar transformation for integration variables ($dx_2 dt \rightarrow J dp_t dy$) which we introduced in our previous work [25] is applied. Therefore we have

$$\frac{d\sigma}{dp_t} = \sum_{i,j} \int J dx_1 dy G_{i/p}(x_1, \mu_f) G_{j/p}(x_2, \mu_f) \frac{d\hat{\sigma}}{dt}, \tag{29}$$

with

$$\begin{aligned}
p_1 &= x_1 \frac{\sqrt{S}}{2} (1, 0, 0, 1), \quad p_2 = x_2 \frac{\sqrt{S}}{2} (1, 0, 0, -1), \\
m_t &= \sqrt{M_\Upsilon^2 + p_t^2}, \quad p_3 = (m_t \cosh y, p_t, 0, m_t \sinh y), \\
x_t &= \frac{2m_t}{\sqrt{S}}, \quad \tau = \frac{m_4^2 - M_\Upsilon^2}{\sqrt{S}}, \\
J &= \frac{4x_1 x_2 p_t}{2x_1 - x_t e^y}, \quad x_2 = \frac{2\tau + x_1 x_t e^{-y}}{2x_1 - x_t e^y}, \\
x_1|_{min} &= \frac{2\tau + x_t e^y}{2 - x_t e^{-y}},
\end{aligned} \tag{30}$$

where \sqrt{S} is the center-of-mass energy of $p\bar{p}(p)$ at Tevatron or LHC, m_4 is the invariant mass of all the final state particles except Υ , and y and p_t are the rapidity and transverse momentum of Υ in the laboratory frame respectively.

V. POLARIZATION

The polarization parameter α is defined as:

$$\alpha(p_t) = \frac{d\sigma_T/dp_t - 2d\sigma_L/dp_t}{d\sigma_T/dp_t + 2d\sigma_L/dp_t}. \tag{31}$$

It represents the measurement of Υ polarization as function of Υ transverse momentum p_t when calculated at each point in p_t distribution. To evaluate $\alpha(p_t)$, the polarization of Υ must be explicitly retained in the calculation. The partonic differential cross section for a polarized Υ is expressed as:

$$\frac{d\hat{\sigma}_\lambda}{dt} = a \epsilon(\lambda) \cdot \epsilon^*(\lambda) + \sum_{i,j=1,2} a_{ij} p_i \cdot \epsilon(\lambda) p_j \cdot \epsilon^*(\lambda), \tag{32}$$

where $\lambda = T_1, T_2, L$. $\epsilon(T_1)$, $\epsilon(T_2)$, $\epsilon(L)$ are the two transverse and longitudinal polarization vectors of Υ respectively, and the polarizations of all the other particles are summed over in n -dimension. One can find that a and a_{ij} are finite when the virtual corrections and real corrections are properly handled as aforementioned. Therefore there is no difference in the differential cross section $d\hat{\sigma}_\lambda/dt$ whether the polarization of Υ is summed over in 4 or n dimensions. Thus we can just treat the polarization vectors of Υ in 4-dimension, and also the spin average factor goes back to 4-dimension. The gauge invariance is explicitly checked by replacing the gluon polarization vector into its 4-momentum in the final numerical calculation.

VI. TREATMENT OF J/ψ

The production mechanism of J/ψ at Tevatron and LHC is much similar to that of Υ except that, color-octet states contribute much more in J/ψ production according to the experimental data and LO theoretical predictions. The results of above calculation can also be applied to the case of J/ψ by doing the substitutions:

$$\begin{aligned}
m_b &\leftrightarrow m_c \\
M_\Upsilon &\leftrightarrow M_{J/\psi} \\
R_s(0)^\Upsilon &\leftrightarrow R_s(0)^{J/\psi} \\
n_f = 4 &\leftrightarrow n_f = 3
\end{aligned} \tag{33}$$

Note that in J/ψ production, charm quark is no longer treated as light quark.

VII. NUMERICAL RESULT

In our numerical computations, the CTEQ6L1 and CTEQ6M PDFs [33], and the corresponding fitted value $\alpha_s(M_Z) = 0.130$ and $\alpha_s(M_Z) = 0.118$ are used for LO and NLO calculations respectively. The bottom quark mass is set as 4.75 GeV.

The choice of the renormalization scale μ_r and factorization scale μ_f is an important issue in the calculations, and it causes uncertainties. We choose $\mu = \mu_r = \mu_f = \sqrt{(2m_b)^2 + p_t^2}$ as our default choice. And the center-of-mass energies are chosen as 1.96 TeV at Tevatron and 14 TeV at LHC.

At First, different values of the two cutoffs, δ_s and δ_c , are used to check the independence of the final results on the cutoffs and the invariance is observed within the error tolerance. Then the two phase space cutoffs are fixed as $\delta_s = 10^{-3}$ and $\delta_c = \delta_s/50$ in the following calculations.

It is known that the QCD perturbative expansion is not good in the regions of small transverse momentum or large rapidity of Υ . Therefore, the results are restricted in the region $p_t > 3$. For the rapidity cut, $|y_\Upsilon| < 1.8$ is chosen at the Tevatron, the same cut condition as the experiments [34], and at the LHC, it is chosen to be $|y| < 3$.

To fix the NRQCD matrix elements for color-octet states of $\Upsilon(1S)$, the D0 data [34] is used, and the fitting starts from Eq.(4) of Ref. [35] where the contributions from spin-singlet states $\eta_b(nS)$ and $h_b(nS)$ are not included. And we have to take a few approximations in our fitting procedure:

- For the S-wave color-singlet part, only the direct color-singlet $\Upsilon(1S)$ and feed-down from $\Upsilon(2S)$ are considered, while other contributions have been neglected. The contribution from the feed-down of $\Upsilon(2S)$ can be included to the direct $\Upsilon(1S)$ production by multiplying a factor of $Br[\Upsilon(2S) \rightarrow \Upsilon(1S) + X] \times \langle \mathcal{O}_1^\Upsilon(2S) \rangle / \langle \mathcal{O}_1^\Upsilon(1S) \rangle$, which results in a factor of 1.127 after a short calculation with PDG data [36]. And the results for direct $\Upsilon(1S)$ of color-singlet contribution are extracted from our previous work [25].
- The contributions from P-wave color-singlet states $\chi_{bJ}(nP)$ are estimated by multiplying a decay fraction $F_{\chi_b(nP)}^{\Upsilon(1S)} \approx F_{\chi_b(1P)}^{\Upsilon(1S)} + F_{\chi_b(2P)}^{\Upsilon(1S)}$, where $F_{\chi_b(1P)}^{\Upsilon(1S)}$ and $F_{\chi_b(2P)}^{\Upsilon(1S)}$ can be obtained from an older sample with the cuts $p_t > 8$ and $|y_\Upsilon| < 0.4$ [37]. As pointed out in Ref. [38], the fraction should not depend very strongly on p_t according to Fig.2 of Ref. [39]. Also, from Fig.4 of Ref. [34] we can see it should not depend very strongly on the rapidity cut either. Thus $F_{\chi_b(1P)}^{\Upsilon(1S)} = 27.1 \pm 6.9 \pm 4.4\%$ and $F_{\chi_b(2P)}^{\Upsilon(1S)} = 10.5 \pm 4.4 \pm 1.4\%$ are taken in our calculation, which result in $F_{\chi_b(nP)}^{\Upsilon(1S)} \approx 37.6 \pm 9.4\%$.

- The contribution from P-wave color-octet states $\Upsilon[{}^3P_J^{(8)}]$ at NLO are still not available. As shown below, the NLO QCD corrections to $\Upsilon[{}^1S_0^{(8)}]$ don't change the cross section very much. If we assume that the NLO QCD corrections to $\Upsilon[{}^3P_J^{(8)}]$ are also small, we can mix it with $\Upsilon[{}^1S_0^{(8)}]$ again, like what we have done at LO. Thus, the value of our fitted $\langle \mathcal{O}_8^\Upsilon({}^1S_0) \rangle_{\text{inc}}$ includes the contributions from $\Upsilon[{}^3P_J^{(8)}]$ as well.

With these approximations, the formula we used for the fitting of inclusive color matrix elements becomes

$$\begin{aligned} d\sigma[\Upsilon]_{\text{inc}} = & 1.127 \times d\sigma[(b\bar{b})_1({}^3S_1)] \langle \mathcal{O}_1^\Upsilon({}^3S_1) \rangle \\ & + F_{\chi_b(nP)}^{\Upsilon(1S)} d\sigma[\Upsilon]_{\text{inc}} + d\sigma[(b\bar{b})_8({}^1S_0)] \langle \mathcal{O}_8^\Upsilon({}^1S_0) \rangle_{\text{inc}} \\ & + d\sigma[(b\bar{b})_8({}^3S_1)] \langle \mathcal{O}_8^\Upsilon({}^3S_1) \rangle_{\text{inc}}, \end{aligned} \quad (34)$$

and the NRQCD matrix elements for color-octet states $\langle \mathcal{O}_8^\Upsilon \rangle_{\text{inc}}$ are determined as

$$\begin{aligned} \langle \mathcal{O}_8^\Upsilon({}^1S_0) \rangle_{\text{inc}} &= (0.948 \pm 0.444) \times 10^{-2} \text{ GeV}^3 \\ \langle \mathcal{O}_8^\Upsilon({}^3S_1) \rangle_{\text{inc}} &= (4.834 \pm 0.719) \times 10^{-2} \text{ GeV}^3, \end{aligned} \quad (35)$$

where only the uncertainty in $F_{\chi_b(nP)}^{\Upsilon(1S)}$ has been considered. The fitting is shown in Fig. 4, together with our prediction for inclusive Υ production at the LHC.

The direct fraction of direct Υ production can also obtained from Ref. [37] as $F_{\text{dir}}^{\Upsilon(1S)} = 50.9 \pm 12.2\%$. Thus we can use the formula

$$\begin{aligned} F_{\text{dir}}^{\Upsilon(1S)} d\sigma[\Upsilon]_{\text{inc}} = & d\sigma[(b\bar{b})_1({}^3S_1)] \langle \mathcal{O}_1^\Upsilon({}^3S_1) \rangle \\ & + d\sigma[(b\bar{b})_8({}^1S_0)] \langle \mathcal{O}_8^\Upsilon({}^1S_0) \rangle \\ & + d\sigma[(b\bar{b})_8({}^3S_1)] \langle \mathcal{O}_8^\Upsilon({}^3S_1) \rangle, \end{aligned} \quad (36)$$

to fit the direct color-octet matrix elements. The matrix elements are obtained as

$$\begin{aligned} \langle \mathcal{O}_8^\Upsilon({}^1S_0) \rangle &= (0.630 \pm 0.576) \times 10^{-2} \text{ GeV}^3 \\ \langle \mathcal{O}_8^\Upsilon({}^3S_1) \rangle &= (3.900 \pm 1.063) \times 10^{-2} \text{ GeV}^3, \end{aligned} \quad (37)$$

where the uncertainty comes only from $F_{\text{dir}}^{\Upsilon(1S)}$. Again the value of our fitted $\langle \mathcal{O}_8^\Upsilon({}^1S_0) \rangle$ includes the contribution from $\Upsilon[{}^3P_J^{(8)}]$. This fitting is shown in Fig. 5, together with our prediction for direct Υ production at the LHC. The band in the figure is obtained from the uncertainty of $F_{\text{dir}}^{\Upsilon(1S)}$.

The dependence of the total cross section on the renormalization scale μ_r and factorization scale μ_f are shown in Fig. 6. It is obvious that the NLO QCD corrections make such dependence milder. We can also see that the NLO QCD corrections effect the cross section lesser at the LHC than at the Tevatron. The p_t distributions of Υ production via S-wave color-octet states are presented

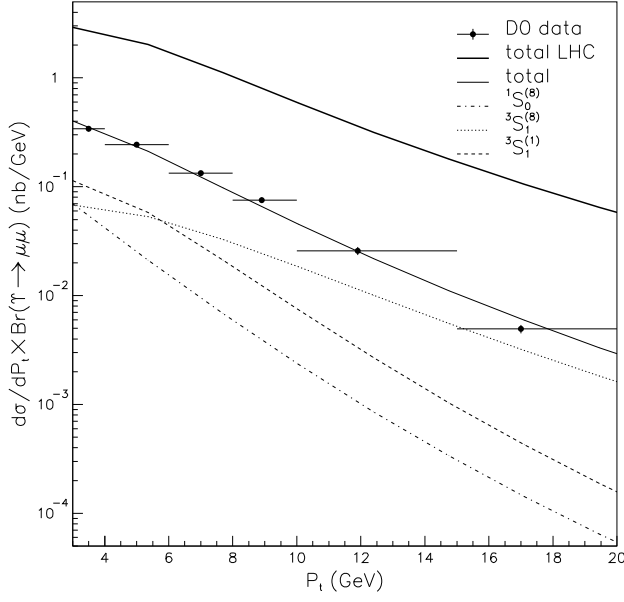


FIG. 4: Transverse momentum distribution of inclusive Υ production at Tevatron and LHC. The D0 data is from Ref. [34].

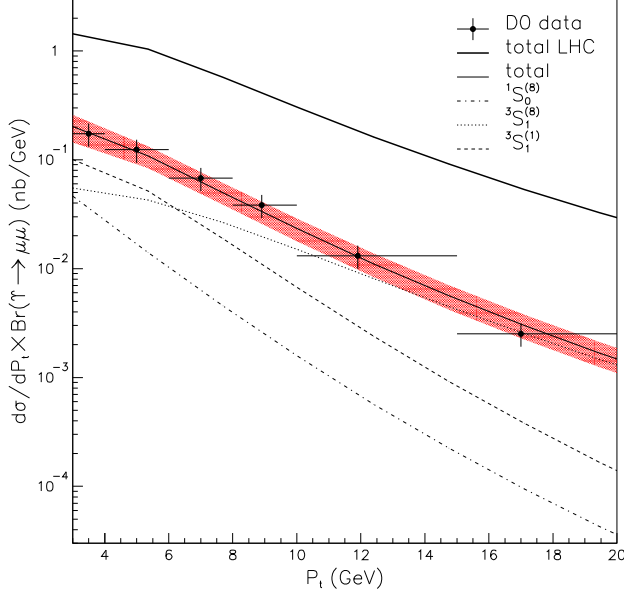


FIG. 5: Transverse momentum distribution of direct Υ production at Tevatron and LHC. The D0 data is from Ref. [34].

in Figs. 7 and 8, where only slight changes appear when the NLO QCD corrections are included.

$\Upsilon[{}^1S_0^{(8)}]$ produces unpolarized Υ , so it contributes to $\alpha = 0$ for both LO and NLO. The p_t distributions of Υ polarization parameter α from $\Upsilon[{}^3S_1^{(8)}]$ are shown in Fig. 9 and there is slight change when the NLO corrections are taken into account. Our predictions for the polarization of direct Υ production are also presented in the figure as a "total" result. In Fig. 10, the polarization of inclusive Υ production at the Tevatron is shown. As

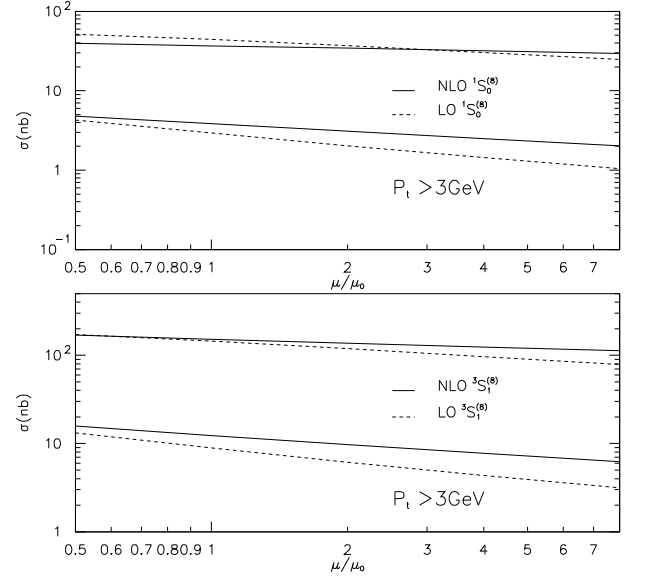


FIG. 6: Total cross section of Υ hadroproduction at LHC (upper curves) and Tevatron (lower curves), as function of μ with $\mu_r = \mu_f = \mu$ and $\mu_0 = \sqrt{(2m_b)^2 + p_t^2}$.

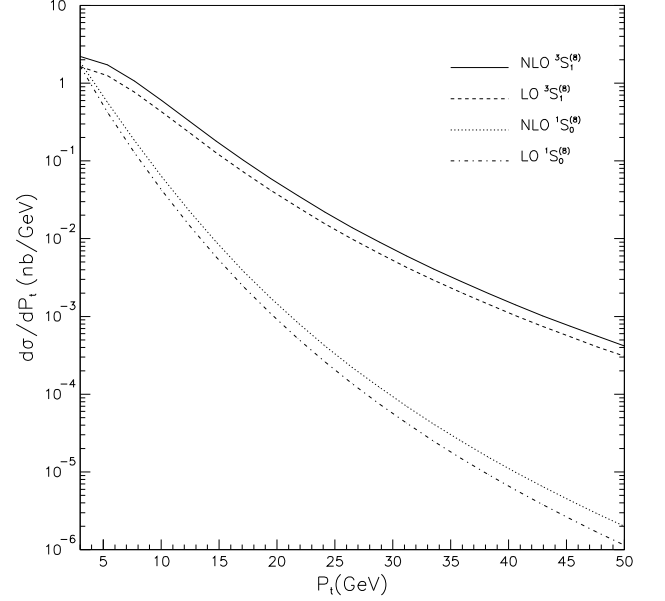


FIG. 7: Transverse momentum distribution of Υ production with $\mu_r = \mu_f = \mu_0$ at the Tevatron.

the polarization of Υ from the feed-down of $\chi_b(nP)$ is not available yet, a huge band is obtained by verifying the polarization of this part between -1 to 1. The experimental data from the D0 is also shown in the same figure. We can see that, there is still some distance between the theoretical prediction and experimental measurement, even with such a large band.

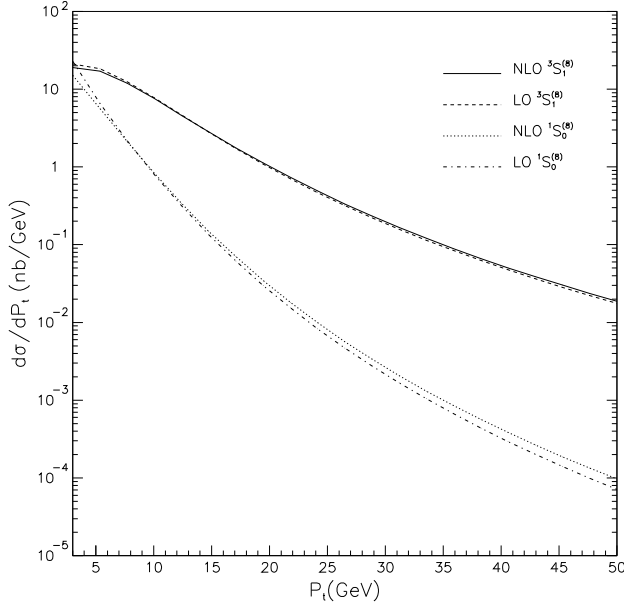


FIG. 8: Transverse momentum distribution of Υ production with $\mu_r = \mu_f = \mu_0$ at the LHC.

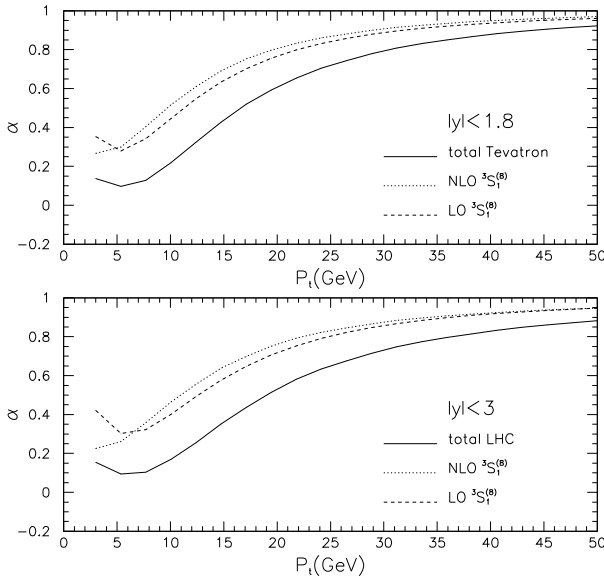


FIG. 9: Transverse momentum distribution of polarization parameter α for direct Υ production at the Tevatron (upper) and LHC (lower).

VIII. SUMMARY AND DISCUSSION

As a summary, in this work, we have calculated the NLO QCD corrections to Υ production via S-wave color-octet states $\Upsilon[{}^1S_0^{(8)}, {}^3S_1^{(8)}]$ at the Tevatron and LHC. With $\mu_r = \mu_f = \mu_0$, the K factors of total cross section (ratio of NLO to LO) are 1.313 and 1.379 for $\Upsilon[{}^1S_0^{(8)}]$ and $\Upsilon[{}^3S_1^{(8)}]$ at Tevatron, while at LHC they are 1.044 and 1.182 respectively. Unlike for the color-singlet case,

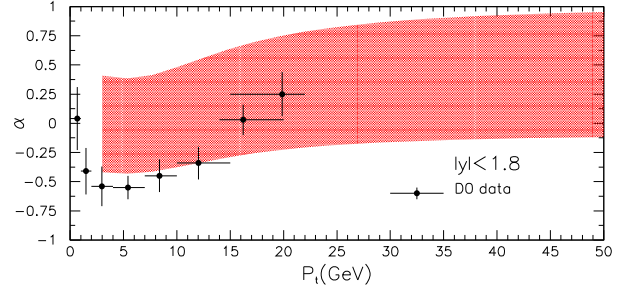


FIG. 10: Transverse momentum distribution of polarization parameter α for inclusive Υ production at the Tevatron. The D0 data is from ref [21].

there are only slight changes to the transverse momentum distributions of Υ production and the Υ polarization when the NLO QCD corrections are taken into account. All the results imply that the perturbative QCD expansion quickly converges for Υ production via the S-wave color-octet states, in contrast with that via color-singlet, where the NLO contributions are too large to hint a good convergence at the NNLO. By fitting the experimental data from the D0 at the Tevatron, the matrix elements for S-wave color-octet states are obtained. And new predictions for the p_t distributions of the Υ production and polarization at the Tevatron and LHC are presented. The prediction for the polarization of inclusive Υ contains large uncertainty rising from the polarization of Υ from feed-down of χ_b . Even with such a large uncertainty, there are still some distance between the prediction and experiment data. Also, the errors of fractions used in the fitting, $F_{\chi_b(1P)}^{\Upsilon(1S)}$, $F_{\chi_b(2P)}^{\Upsilon(1S)}$ and $F_{\text{dir}}^{\Upsilon(1S)}$, are quite large and result large uncertainty in the matrix elements. New measurements on the production and also polarization for direct Υ are expected. This would make the matrix elements more precise, and get rid of the large uncertainty from χ_b .

This work is supported by the National Natural Science Foundation of China (No. 10475083, 10979056 and 10935012), by the Chinese Academy of Science under Project No. INFO-115-B01, and by the China Postdoctoral Science foundation No. 20090460535.

Appendix A: Calculation of the factor I^{jk}

If we write the n -momentum of soft gluon in the $p_1 + p_2$ rest frame as

$$p_5 = E_5(1, \dots, \sin \theta_1 \cos \theta_2, \cos \theta_1), \quad (\text{A1})$$

then I^{jk} is defined as

$$I^{jk} = \int \frac{-(p_j \cdot p_k)}{(p_j \cdot p_5)(p_k \cdot p_5)} dS, \quad (\text{A2})$$

with

$$dS = \frac{1}{\pi} \left(\frac{4}{s_{12}} \right)^{-\epsilon} \int_0^{\delta_s \sqrt{s_{12}}/2} dE_5 E_5^{1-2\epsilon} \sin^{1-2\epsilon} \theta_1 d\theta_1 \\ \times \sin^{-2\epsilon} \theta_2 d\theta_2. \quad (\text{A3})$$

Before the calculation of I^{jk} , define β_j as $\beta_j = |\vec{p}_j|/E_j$, which is the ratio of momentum to energy of particle i in the $p_1 + p_2$ rest frame, where

$$\beta_1 = \beta_2 = \beta_4 = 1, \quad \beta_3 = \frac{\hat{s} - 1}{\hat{s} + 1} \equiv \beta. \quad (\text{A4})$$

Then we can write p_j and p_k as

$$p_j = E_j(1, \dots, \beta_j) \\ p_k = E_k(1, \dots, \beta_k \sin \theta_{jk}, \beta_k \cos \theta_{jk}), \quad (\text{A5})$$

where θ_{jk} is the angel between j and k . Now we have

$$I^{jk} = -\frac{1 - \beta_j \beta_k \cos \theta}{\pi} I_E I_A^{jk}, \quad (\text{A6})$$

where

$$I_E = \left(\frac{4}{s_{12}} \right)^{-\epsilon} \int_0^{\delta_s \sqrt{s_{12}}/2} dE_5 E_5^{-1-2\epsilon} \\ = \left(-\frac{1}{2\epsilon} \right) (\delta_s)^{-2\epsilon}, \quad (\text{A7})$$

and

$$I_A^{jk} = \int_0^\pi \sin^{1-2\epsilon} \theta_1 d\theta_1 \int_0^\pi \sin^{-2\epsilon} \theta_2 d\theta_2 \frac{1}{1 - \beta_j \cos \theta_1} \\ \times \frac{1}{1 - \beta_k \cos \theta \cos \theta_1 - \beta_k \sin \theta \sin \theta_1 \cos \theta_2}. \quad (\text{A8})$$

The way to calculate the integrals I_A^{jk} can be found in the appendix of Ref. [31]. Now we come to the results. It's easily to obtain

$$I^{11} = I^{22} = I^{44} = 0, \quad (\text{A9})$$

and the others are listed below.

1. I^{1i} with $i = 2, 3, 4$. Write the momenta of the particles as

$$p_1 = E_1(1, \dots, 1), \\ p_2 = E_2(1, \dots, -1), \\ p_3 = E_3(1, \dots, \beta \sin \theta_{13}, \beta \cos \theta_{13}), \\ p_4 = E_4(1, \dots, -\sin \theta_{13}, -\cos \theta_{13}), \quad (\text{A10})$$

then we have

$$I_A^{12} = -\frac{\pi}{\epsilon}, \\ I_A^{13} = \frac{\pi}{1 - \beta \cos \theta_{13}} \left\{ -\frac{1}{\epsilon} + \ln \frac{(1 - \hat{t})^2}{\hat{s}} - \epsilon \left[\ln^2(1 - \hat{t}) \right. \right. \\ \left. \left. - \frac{1}{2} \ln^2 \hat{s} + 2\text{Li}_2(\hat{t}) - 2\text{Li}_2\left(\frac{\hat{u}}{1 - \hat{t}}\right) \right] \right\}, \quad (\text{A11}) \\ I_A^{14} = -\frac{2\pi}{(1 + \cos \theta_{13})\epsilon} \left(\frac{\hat{u}}{1 - \hat{s}} \right)^{-\epsilon} \left[1 + \epsilon^2 \text{Li}_2\left(\frac{\hat{t}}{1 - \hat{s}}\right) \right],$$

which lead to

$$I^{12} = -\frac{2}{\pi} I_E I_A^{12} = -\frac{1}{\epsilon^2} \delta_s^{-2\epsilon} \\ I^{13} = -\frac{1 - \beta \cos \theta_{13}}{\pi} I_E I_A^{13} \\ = -\frac{1}{2\epsilon^2} \delta_s^{-2\epsilon} \left\{ 1 - \epsilon \ln \frac{(1 - \hat{t})^2}{\hat{s}} + \epsilon^2 \left[\ln^2(1 - \hat{t}) \right. \right. \\ \left. \left. - \frac{1}{2} \ln^2 \hat{s} + 2\text{Li}_2(\hat{t}) - 2\text{Li}_2\left(\frac{\hat{u}}{1 - \hat{t}}\right) \right] \right\}, \\ I^{14} = -\frac{1 + \cos \theta_{13}}{\pi} I_E I_A^{14} \\ = -\frac{1}{\epsilon^2} \delta_s^{-2\epsilon} \left(\frac{\hat{u}}{1 - \hat{s}} \right)^{-\epsilon} \left[1 + \epsilon^2 \text{Li}_2\left(\frac{\hat{t}}{1 - \hat{s}}\right) \right]. \quad (\text{A12})$$

2. I^{2i} with $i = 3, 4$. These two can be directly obtained from I_{1i} with the substitution $\hat{t} \leftrightarrow \hat{u}$.

$$I^{23} = -\frac{1}{2\epsilon^2} \delta_s^{-2\epsilon} \left\{ 1 - \epsilon \ln \frac{(1 - \hat{u})^2}{\hat{s}} + \epsilon^2 \left[\ln^2(1 - \hat{u}) \right. \right. \\ \left. \left. - \frac{1}{2} \ln^2 \hat{s} + 2\text{Li}_2(\hat{u}) - 2\text{Li}_2\left(\frac{\hat{t}}{1 - \hat{u}}\right) \right] \right\}, \\ I^{24} = -\frac{1}{\epsilon^2} \delta_s^{-2\epsilon} \left(\frac{\hat{t}}{1 - \hat{s}} \right)^{-\epsilon} \left[1 + \epsilon^2 \text{Li}_2\left(\frac{\hat{u}}{1 - \hat{s}}\right) \right].$$

3. I^{33} and I^{34} . Write the momenta of the final state particles as

$$p_3 = E_3(1, \dots, -\beta), \\ p_4 = E_4(1, \dots, 1), \quad (\text{A13})$$

then

$$I_A^{33} = \frac{2\pi}{1 - \beta^2} \left[1 + \epsilon \frac{1}{\beta} \ln \hat{s} \right], \\ I_A^{34} = \frac{\pi}{1 + \beta} \left\{ -\frac{1}{\epsilon} + \ln \hat{s} - \epsilon \left[\frac{1}{2} \ln^2 \hat{s} + 2\text{Li}_2(1 - \hat{s}) \right] \right\}, \\ I^{33} = -\frac{1 - \beta^2}{\pi} I_E I_A^{33} = \frac{1}{\epsilon} \delta_s^{-2\epsilon} \left[1 + \epsilon \frac{1}{\beta} \ln \hat{s} \right], \\ I^{34} = -\frac{1 + \beta}{\pi} I_E I_A^{34} \\ = -\frac{1}{2\epsilon^2} \delta_s^{-2\epsilon} \left\{ 1 - \epsilon \ln \hat{s} + \epsilon^2 \left[\frac{1}{2} \ln^2 \hat{s} + 2\text{Li}_2(1 - \hat{s}) \right] \right\}. \quad (\text{A14})$$

Appendix B: Color Factors

Here we present color factors for all the processes involved. Color indices for particle n are labeled as j_n .

1. LO processes

The color factors listed here for LO processes have been orthogonalized and normalized.

- $gg \rightarrow \Upsilon[S_0^{(8)}]g$, three color factors in total:

$$\begin{aligned} & \frac{1}{\sqrt{5}} \text{Tr}[T^{j_4} T^{j_2} T^{j_1} T^{j_3} - T^{j_4} T^{j_3} T^{j_1} T^{j_2}], \\ & \frac{1}{\sqrt{5}} \text{Tr}[T^{j_4} T^{j_3} T^{j_2} T^{j_1} - T^{j_4} T^{j_1} T^{j_2} T^{j_3}], \\ & \frac{1}{\sqrt{5}} \text{Tr}[T^{j_4} T^{j_2} T^{j_3} T^{j_1} - T^{j_4} T^{j_1} T^{j_3} T^{j_2}]. \end{aligned} \quad (\text{B1})$$

- $gg \rightarrow \Upsilon[S_1^{(8)}]g$, three color factors also:

$$\begin{aligned} & \frac{1}{3\sqrt{2}} \text{Tr}[(T^{j_4} T^{j_2} T^{j_3} T^{j_1} + T^{j_4} T^{j_1} T^{j_3} T^{j_2}) \\ & \quad - (T^{j_4} T^{j_1} T^{j_2} T^{j_3} + T^{j_4} T^{j_3} T^{j_2} T^{j_1})], \\ & \frac{1}{3\sqrt{6}} \text{Tr}[(T^{j_4} T^{j_2} T^{j_3} T^{j_1} + T^{j_4} T^{j_1} T^{j_3} T^{j_2}) \\ & \quad + (T^{j_4} T^{j_1} T^{j_2} T^{j_3} + T^{j_4} T^{j_3} T^{j_2} T^{j_1}) \\ & \quad - 2(T^{j_4} T^{j_2} T^{j_1} T^{j_3} + T^{j_4} T^{j_3} T^{j_1} T^{j_2})], \\ & \frac{1}{\sqrt{15}} \text{Tr}[(T^{j_4} T^{j_2} T^{j_3} T^{j_1} + T^{j_4} T^{j_1} T^{j_3} T^{j_2}) \\ & \quad + (T^{j_4} T^{j_1} T^{j_2} T^{j_3} + T^{j_4} T^{j_3} T^{j_2} T^{j_1}) \\ & \quad + (T^{j_4} T^{j_2} T^{j_1} T^{j_3} + T^{j_4} T^{j_3} T^{j_1} T^{j_2})]. \end{aligned} \quad (\text{B2})$$

- $gq \rightarrow \Upsilon[S_0^{(8)}]q$, only one color factor:

$$\frac{1}{2\sqrt{15}} [3(T^{j_1} T^{j_3} + T^{j_3} T^{j_1})_{j_4 j_2} - \delta_{j_4 j_2} \delta_{j_1 j_3}]. \quad (\text{B3})$$

- $gq \rightarrow \Upsilon[S_1^{(8)}]q$, two color factors:

$$\frac{\sqrt{3}}{4} (T^{j_3} T^{j_1})_{j_4 j_2}, -\frac{1}{4\sqrt{21}} (8T^{j_1} T^{j_3} + T^{j_3} T^{j_1})_{j_4 j_2}. \quad (\text{B4})$$

- $q\bar{q} \rightarrow \Upsilon^{(8)}g$, almost same with $gq \rightarrow \Upsilon^{(8)}q$.

2. Virtual correction processes

In the amplitude of virtual correction processes, besides the same color factors as in the corresponding LO process, there are extra ones. As we have mentioned before, virtual correction to the cross section is related to virtual amplitude as Eq.(6). Then the terms in proportion to these extra color factors will vanish and do not contribute to the final result as we have orthogonalized the color factors of LO processes. Thus no new color factors in virtual correction processes need to be presented here.

3. Real correction processes

In order to present the color factors of real correction processes in a simplified form, we list here all independent color factors in a certain process. Actually in our calculation, they are orthogonalized and normalized too, which are too complicated to be listed here.

- $gg \rightarrow \Upsilon[S_0^{(8)}]gg$, twelve color factors. The permutations of j_1, j_2, j_3 and j_4 contain 24 terms. Divide them into twelve groups with two terms in each group, and the twelve color factors can be expressed as

$$\text{Tr}[T^{j_5} (T^a T^b T^c T^d + T^d T^c T^b T^a)], \quad (\text{B5})$$

where a, b, c, d are permutations of j_1, j_2, j_3 and j_4 .

- $gg \rightarrow \Upsilon[S_1^{(8)}]gg$, also twelve color factors. They can be expressed as

$$\text{Tr}[T^{j_5} (T^a T^b T^c T^d - T^d T^c T^b T^a)], \quad (\text{B6})$$

- $gg \rightarrow \Upsilon[S_0^{(8)}]q\bar{q}$, five independent color factors:

$$\begin{aligned} & d^{j_2 j_3 k} (T^{j_1} T^k)_{j_4 j_5}, \quad d^{j_2 j_3 k} (T^k T^{j_1})_{j_4 j_5}, \\ & d^{j_1 j_3 k} (T^{j_2} T^k)_{j_4 j_5}, \quad d^{j_1 j_3 k} (T^k T^{j_2})_{j_4 j_5}, \\ & 6(T^{j_3} T^{j_2} T^{j_1} - T^{j_1} T^{j_2} T^{j_3})_{j_4 j_5} + i f^{j_1 j_2 j_3} \delta_{j_4 j_5}. \end{aligned} \quad (\text{B7})$$

- $gg \rightarrow \Upsilon[S_1^{(8)}]q\bar{q}$, seven independent color factors. One is $d^{j_1 j_2 j_3} \delta_{j_4 j_5}$ while the others can be expressed as

$$(T^a T^b T^c)_{j_4 j_5}, \quad (\text{B8})$$

where a, b, c are permutations of j_1, j_2 and j_3 .

- $gq \rightarrow \Upsilon^{(8)}gq$ and $q\bar{q} \rightarrow \Upsilon^{(8)}gg$, similar to $gg \rightarrow \Upsilon^{(8)}q\bar{q}$.

- $q\bar{q} \rightarrow \Upsilon[S_0^{(8)}]q\bar{q}$, two color factors:

$$T_{j_2 j_5}^{j_3} \delta_{j_4 j_1} + T_{j_4 j_1}^{j_3} \delta_{j_2 j_5}, \quad T_{j_2 j_1}^{j_3} \delta_{j_4 j_5} + T_{j_4 j_5}^{j_3} \delta_{j_2 j_1}. \quad (\text{B9})$$

- $q\bar{q} \rightarrow \Upsilon[S_1^{(8)}]q\bar{q}$, four color factors:

$$T_{j_2 j_5}^{j_3} \delta_{j_4 j_1}, \quad T_{j_4 j_1}^{j_3} \delta_{j_2 j_5}, \quad T_{j_2 j_1}^{j_3} \delta_{j_4 j_5}, \quad T_{j_4 j_5}^{j_3} \delta_{j_2 j_1}. \quad (\text{B10})$$

- $qq \rightarrow \Upsilon^{(8)}qq$, similar to $q\bar{q} \rightarrow \Upsilon^{(8)}q\bar{q}$.

- $q\bar{q} \rightarrow \Upsilon[S_0^{(8)}]q'\bar{q}'$, only one color factor:

$$3(T_{j_2 j_5}^{j_3} \delta_{j_4 j_1} + T_{j_4 j_1}^{j_3} \delta_{j_2 j_5}) - 2(T_{j_2 j_1}^{j_3} \delta_{j_4 j_5} + T_{j_4 j_5}^{j_3} \delta_{j_2 j_1}). \quad (\text{B11})$$

- $q\bar{q} \rightarrow \Upsilon[S_1^{(8)}]q'\bar{q}'$, three color factor:

$$\begin{aligned} & T_{j_2 j_5}^{j_3} \delta_{j_4 j_1} - T_{j_4 j_1}^{j_3} \delta_{j_2 j_5}, \\ & T_{j_2 j_1}^{j_3} \delta_{j_4 j_5} - T_{j_4 j_5}^{j_3} \delta_{j_2 j_1}, \\ & 3T_{j_4 j_1}^{j_3} \delta_{j_2 j_5} - T_{j_4 j_5}^{j_3} \delta_{j_2 j_1}. \end{aligned} \quad (\text{B12})$$

- $qq' \rightarrow \Upsilon^{(8)}qq'$, similar to $q\bar{q} \rightarrow \Upsilon^{(8)}q'\bar{q}'$.

-
- [1] E. Braaten and S. Fleming, Phys. Rev. Lett. **74**, 3327 (1995).
- [2] G. T. Bodwin, E. Braaten, and G. P. Lepage, Phys. Rev. **D51**, 1125 (1995).
- [3] . Kramer, Michael, Prog. Part. Nucl. Phys. **47**, 141 (2001), hep-ph/0106120.
- [4] J. P. Lansberg, Int. J. Mod. Phys. **A21**, 3857 (2006), hep-ph/0602091.
- [5] K. Abe *et al.* [BELLE Collaboration], Phys. Rev. Lett. **88**, 052001 (2002); K. Abe *et al.* [Belle Collaboration], Phys. Rev. Lett. **89**, 142001 (2002); K. Abe *et al.* [Belle Collaboration], Phys. Rev. D **70**, 071102 (2004); P. Pakhlov *et al.* [Belle Collaboration], Phys. Rev. D **79**, 071101 (2009).
- [6] B. Aubert *et al.* [BABAR Collaboration], Phys. Rev. D **72**, 031101 (2005).
- [7] Y. J. Zhang, Y. j. Gao and K. T. Chao, Phys. Rev. Lett. **96**, 092001 (2006); Y. J. Zhang and K. T. Chao, Phys. Rev. Lett. **98**, 092003 (2007); Y. J. Zhang, Y. Q. Ma and K. T. Chao, Phys. Rev. D **78**, 054006 (2008); Y. Q. Ma, Y. J. Zhang and K. T. Chao, Phys. Rev. Lett. **102**, 162002 (2009); B. Gong and J. X. Wang, Phys. Rev. D **77**, 054028 (2008); B. Gong and J. X. Wang, Phys. Rev. Lett. **100**, 181803 (2008); B. Gong and J. X. Wang, Phys. Rev. Lett. **102**, 162003 (2009); W. L. Sang and Y. Q. Chen, arXiv:0910.4071 [hep-ph]; D. Li, Z. G. He and K. T. Chao, Phys. Rev. D **80**, 114014 (2009); Y. J. Zhang, Y. Q. Ma, K. Wang and K. T. Chao, Phys. Rev. D **81**, 034015 (2010).
- [8] B. Gong and J. X. Wang, Phys. Rev. D **80**, 054015 (2009).
- [9] G. T. Bodwin, D. Kang, T. Kim, J. Lee and C. Yu, AIP Conf. Proc. **892**, 315 (2007); Z. G. He, Y. Fan and K. T. Chao, Phys. Rev. D **75**, 074011 (2007); G. T. Bodwin, J. Lee and C. Yu, Phys. Rev. D **77**, 094018 (2008); Z. G. He, Y. Fan and K. T. Chao, Phys. Rev. D **81**, 054036 (2010); Y. Jia, arXiv:0912.5498 [hep-ph].
- [10] S. J. Brodsky and J. P. Lansberg, Phys. Rev. D **81**, 051502 (2010); J. P. Lansberg, arXiv:1003.4319 [hep-ph].
- [11] Y. Q. Ma, K. Wang and K. T. Chao, arXiv:1002.3987 [hep-ph].
- [12] M. I. Kramer, Nucl. Phys. B **459**, 3 (1996).
- [13] P. Artoisenet, J. M. Campbell, F. Maltoni and F. Tramontano, Phys. Rev. Lett. **102**, 142001 (2009); C. H. Chang, R. Li and J. X. Wang, Phys. Rev. D **80**, 034020 (2009).
- [14] M. Butenschoen and B. A. Kniehl, Phys. Rev. Lett. **104**, 072001 (2010).
- [15] R. Li and J. X. Wang, Phys. Lett. B **672**, 51 (2009); J. P. Lansberg, Phys. Lett. B **679**, 340 (2009).
- [16] Z. G. He, R. Li and J. X. Wang, arXiv:0904.1477 [hep-ph]; Z. G. He, R. Li and J. X. Wang, Phys. Rev. D **79**, 094003 (2009).
- [17] Z. G. He and J. X. Wang, Phys. Rev. D **81**, 054030 (2010).
- [18] R. Li, Y. J. Zhang and K. T. Chao, Phys. Rev. D **80**, 014020 (2009) [arXiv:0903.2250 [hep-ph]]. C. F. Qiao, L. P. Sun and P. Sun, J. Phys. G **37**, 075019 (2010) [arXiv:0903.0954 [hep-ph]]. P. Ko, C. Yu and J. Lee, arXiv:1006.3846 [hep-ph]. P. Ko, C. Yu and J. Lee, arXiv:1007.3095 [hep-ph].
- [19] R. Li and J. X. Wang, arXiv:1007.2368 [hep-ph].
- [20] A. Abulencia *et al.* (CDF), Phys. Rev. Lett. **99**, 132001 (2007).
- [21] V. M. Abazov *et al.* (D0), Phys. Rev. Lett. **101**, 182004 (2008), 0804.2799.
- [22] E. Braaten and J. Lee, Phys. Rev. **D63**, 071501 (2001), hep-ph/0012244.
- [23] J. Campbell, F. Maltoni, and F. Tramontano, Phys. Rev. Lett. **98**, 252002 (2007).
- [24] B. Gong and J.-X. Wang, Phys. Rev. Lett. **100**, 232001 (2008), 0802.3727.
- [25] B. Gong and J.-X. Wang, Phys. Rev. **D78**, 074011 (2008), 0805.2469.
- [26] C.-F. Qiao and J.-X. Wang, Phys. Rev. **D69**, 014015 (2004).
- [27] P. Artoisenet, J. P. Lansberg, and F. Maltoni, Phys. Lett. **B653**, 60 (2007).
- [28] B. Gong, X. Q. Li, and J.-X. Wang, Phys. Lett. **B673**, 197 (2009), 0805.4751.
- [29] P. L. Cho and A. K. Leibovich, Phys. Rev. **D53**, 6203 (1996), hep-ph/9511315.
- [30] M. Klasen, B. A. Kniehl, L. N. Mihaila, and M. Steinhauser, Nucl. Phys. **B713**, 487 (2005).
- [31] B. W. Harris and J. F. Owens, Phys. Rev. **D65**, 094032 (2002).
- [32] G. Altarelli, R. K. Ellis, and G. Martinelli, Nucl. Phys. **B157**, 461 (1979).
- [33] J. Pumplin *et al.*, JHEP **07**, 012 (2002), hep-ph/0201195.
- [34] V. M. Abazov *et al.* (D0), Phys. Rev. Lett. **94**, 232001 (2005), hep-ex/0502030.
- [35] E. Braaten, S. Fleming, and A. K. Leibovich, Phys. Rev. **D63**, 094006 (2001), hep-ph/0008091.
- [36] C. Amsler *et al.* (Particle Data Group), Phys. Lett. **B667**, 1 (2008).
- [37] T. Affolder *et al.* (CDF), Phys. Rev. Lett. **84**, 2094 (2000), hep-ex/9910025.
- [38] P. Artoisenet, J. M. Campbell, J. P. Lansberg, F. Maltoni, and F. Tramontano, Phys. Rev. Lett. **101**, 152001 (2008), 0806.3282.
- [39] D. E. Acosta *et al.* (CDF), Phys. Rev. Lett. **88**, 161802 (2002).